Journal of Nuclear Materials 392 (2009) 427–433

Contents lists available at ScienceDirect

Journal of Nuclear Materials

journal homepage: www.elsevier.com/locate/jnucmat

Experimental and theoretical investigation of sorption kinetics of beryllium on Amberlite-IR-120 sorbent

Sameh H. Othman [a], M. Shabaan [b], M. Demerdash [b], Mahmoud M. Saleh [c,*]

[a] *Nuclear Research Center, Atomic Energy Authority, Cairo, Egypt*
[b] *Nuclear Materials Authority, Cairo, Egypt*
[c] *Chemistry Dept., Faculty of science, Cairo University, Cairo, Egypt*

ARTICLE INFO

Article history:
Received 24 October 2008
Accepted 1 April 2009

ABSTRACT

Experimental and theoretical studies of the sorption kinetics of beryllium cation from its synthetic solution on amberlite IR-120 (Amb-IR-120) sorbent was achieved at different temperatures. The dependence of the sorption kinetic parameters on the temperature of the solution has been investigated. The pH of solution and agitation speed had dramatic effects on the uptake of Be by Amb-IR-120. It was found that pH in the range of 3–3.5 and agitation speed of 150 rpm are proper conditions of Be sorption at the present experimental set. The fit of experimental data with the homogeneous diffusion model (HDM) equations demonstrated the possibility of using this model for adequate description of the beryllium sorption kinetics on the Amb-IR-120 sorbent. Two stages of adsorption with different controlling processes were proposed. Liquid film diffusion controls the process at the early stage of the adsorption followed by matrix diffusion which controls the process in the final stage. Two different equations were used to express each stage.

1. Introduction

Beryllium is a unique metal with exceptional material properties. Due to it's highly desirable material properties it has become an essential element used in the aerospace, computer, electronics and nuclear industries [1,2]. Whereas beryllium oxide acts as an electrical insulator in some applications, beryllium presents an essential constituent of synthetic optical crystals as $La_2Be_2O_5$, $BeAl_2O_4$, $BeAl_6O_{10}$ and $LaBeAl_{11}O_{19}$ which possess good potentials as effective laser materials [3–6]. Based on its high melting point (~1285 °C), low neutron absorption and high scattering cross sections [7] beryllium was used in nuclear reactors as effective neutron reflector and moderator [8]. When bombarded by alpha particles it becomes a useful source of neutrons. It also has the property of being able to reflect, slow down and capture neutrons, and so the metal and metal oxides are widely used as a moderator in nuclear reactor control rods. Its ability to reflect neutrons has also made it useful in the casings for nuclear bombs where, in the early stages of detonation, it reflects neutrons back into the chain reaction [9].

The contents of beryllium in the earth's crust [10], in soil [11] and in coal [12] are about 2–6, 1.2–2.1 and 2.5 $\mu g\ g^{-1}$, respectively. The aforementioned sources of Be compounds and by aid of rains [13,14] may dissolve in water [15] and contaminate the sources of water and present in the sediments [16]. Due to their unique properties, beryllium and its metal alloys (such as Cu, Al, Mg, Ni) have been widely used for electrical equipment, electronic instrumentation, structural components for aircraft, missiles and satellites [17,18]. Beryllium and its compounds are highly toxic and may cause lung disease (berylliosis) [17,18], eye and mucous membrane irritation, fatigue and weight loss, and is probably a human carcinogen [19,20]. Hence, beryllium is classified by USEPA in Group B2 [20]. However the studies on removal Be containing compounds are few compared to the huge number of literatures concerning other metals.

Beryllium can strongly be adsorbed on the cation exchange resin Amberlite IR-120 which can be recovered by elution with hydrochloric acid [21,22]. This separation principle, based on absorbability of beryllium on Amberlite IR-120 from an EDTA solution of pH 3.5, has been used for the determination of beryllium in beryl [23] and in aluminum metal and alloy's [24]. Ion exchange process was developed for treating the liquor prepared from Egyptian beryl in order to separate Be from Al, Fe and other deleterious impurities. However, the application of these systems in industrial scale equipment using fixed column or fluidized bed technology requires a knowledge of the equilibrium and kinetics of the metal extraction processes and the operating hydrodynamic behavior. The determination of the kinetic parameters has two objectives: (i) to approach, as accurately as possible, the real physical chemistry of the metal extraction process and (ii) to get empirical or semi-empirical equations for the design of the equipment. So, this study

---

* Corresponding author.
E-mail address: mahmoudsaleh90@yahoo.com (M.M. Saleh).

0022-3115/$ - see front matter © 2009 Elsevier B.V. All rights reserved.
doi:10.1016/j.jnucmat.2009.04.001

Nomenclature

C_o	initial concentration of sorbing species, M
C_e	equilibrium concentration of sorbing species, M
D_{MD}	diffusion coefficient in solid phase, $m^2\ s^{-1}$
D_{FD}	diffusion coefficient in liquid phase, $m^2\ s^{-1}$
E_a	activation energy, kJ/mol
k	pseudo first order rate constant, min^{-1}
k_l	Lagergren sorption rate constant, min^{-1}
k_s	the second order rate constant, $g\ mg^{-1}\ min^{-1}$
K_{FD}	liquid film diffusion constant
K_{MD}	matrix diffusion constant
m	the weight of the resin, g
n, y	stoichiometric coefficients
q_e	amount of solute sorbed at equilibrium, $mg\ g^{-1}$
q_t	amount of solute sorbed at time t, $mg\ g^{-1}$
R	gas constant, 82.06 (cm^3 atm)/(mol/K)
r	average particle radius, m
X	fractional attainment of equilibrium or extent of solid conversion
T	absolute temperature, K
t	time, min
U	uptake percent
V	volume of solution, cm^3
δ	liquid film thickness, m

is aimed to investigate the sorption kinetics of beryllium cation from its synthetic solution on Amb-IR-120 sorbent.

Although the kinetics of adsorption of different metals on Amberlite-120 has been extensively investigated, the adsorption of beryllium on Amberlyite-120 remain limited [25,26]. For this purpose homogeneous diffusion model will be examined to simulate the adsorption process of beryllium on Amb-IR-120 resin to attain more knowledge about the mechanism, equilibrium and kinetics of the adsorption process of beryllium.

2. Experimental

2.1. Materials

All chemicals used in this study were of analytical grade reagent and were used as received. Amb-IR-120, (Aldrich product) its matrix component is styrene–divinyl benzene (gel type) and the matrix active group is sulfonic acid. The beryllium sulphate was obtained from Fluka.

2.2. Sorption kinetics

Batch sorption studies were performed by mixing 0.8 g dry resin particles with 100 mL Beryllium sulphate $BeSO_4{\cdot}4H_2O$ solution of 1.10×10^{-2} M initial concentration in a 250 mL stopper conical flask. The mixtures were shaken in a thermostatic shaker at different temperatures (31–65 °C) for 2 h. Aliquot samples were taken from the flask at appropriate time intervals as necessary and the concentration of beryllium was determined using a Unicam AA spectrometer, model 969. An investigation of the effect of solution pH on beryllium sorption was performed to determine a proper pH range at which maximum uptake of metal can be achieved. The process was evaluated using the sorbent in a pH range of 2–5 and adjusted when necessary, with 0.1 M HCl and/or 0.1 M NaOH solutions using a Jenway pH meter.

After the sorbent is saturated with beryllium it is eluted with HCl. The amount of Be(II) sorbed onto the resin (q, $mg\ g^{-1}$) and the uptake percent ($U\%$) were respectively determined using the following relations [27]:

$$q = (C_0 - C_e)\frac{V}{m} \tag{1}$$

$$U\% = \frac{(C_0 - C_e)}{C_e} X100 \tag{2}$$

where C_0 and C_e are the initial and equilibrium concentrations of Be(II) in the solution ($mol\ L^{-1}$), V is the volume of solution (L), m is the weight of the resin (g). All experiments were performed at pH of 3.5 in duplicate and the averaged values were taken.

3. Results and discussion

3.1. Sorption performance

The affinity of Amb-IR-120 resins towards Be(II) was tested by adsorption of beryllium upon Amb-IR-120 in a batch reactor at temperature 31 °C. As shown in Fig. 1, the uptake percent increases with time until it reaches a plateau. The absorbability of the amberlite resin towards the beryllium ions increases with the temperature (see Fig. 3). The ion exchange of metal ions involves the formation of different mixed species in the resin phase depending on the pH. The pH value of the working system plays an important role on sorption extent because of its influence on the degree of ionization and the surface properties of the applied sorbents. The speciation of beryllium ions in aqueous solution could be described by the following reaction:

$$Be^{2+} + (2+n-y)HAmb + yL^- \Longleftrightarrow BeL_yAmb_{(2-y)}HAmb_{(n)} + (2-y)H^+ \tag{3}$$

The variation in the removal extent of Be(II) with pH using Amb-IR-120 was studied by batch experiment and shown in Fig. 2. As it was expected, the solution pH greatly affects the sorption of Be(II) in accordance with the proposed specification equation above. As the pH increases the amount adsorbed increases before it decreases again at pH >3.5. The last observation can be attributed to the hydrolysability of the Be^{2+} ions, a process which decreases the absorbability of the beryllium ions.

The above results lead us to re-write the above equation at pH 3.5 to be as follow:

$$[Be(H_2O)_4]^{2+} + (2+n)HAmb \Longleftrightarrow BeAmb_2(H_2O)_2(HAmb)_n + 2[H_3O]^+ \tag{4}$$

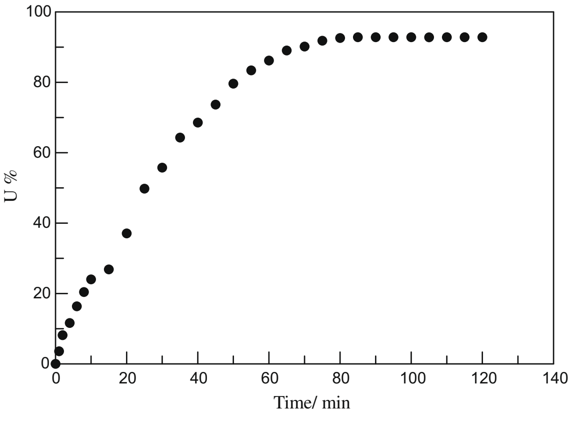

Fig. 1. Uptake percent of beryllium from a synthetic solution on Amb-IR-120 resin. Amount of resin 0.8 g, shaking speed 150 rpm at 31 °C.

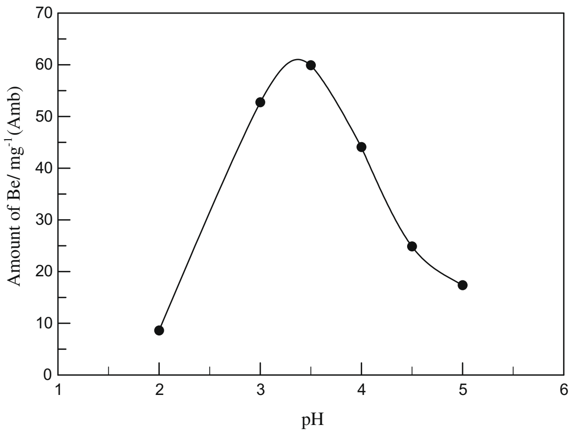

Fig. 2. Effect of pH on the adsorption of Be on Amb-IR-120 resin. Amount of resin 0.8 g, shaking speed 150 rpm at 31 °C.

The stability constant of the complex according to the indicated reaction was determined experimentally to be 1.3×10^3 at a pH of 3.26. As evident from Eq. (4), the pH has a dramatic effects on the adsorption extent of Be(II) on Amb-IR-120. The pH influences the degree of ionization of the reactive acidic group of the resin. Since maximum sorption occurs at pH 3.5, this pH was taken as the optimum value for all sorption studies at the present experimental conditions.

3.2. Sorption kinetics and mechanism

The data obtained from batch experiments which performed at different temperatures (31–65) °C are evaluated by using the simple Lagergren equation [28] to determine the rate of the sorptive interactions assuming pseudo first order kinetics

$$\log(q_e - q_t) = \log q_e \frac{-k_l t}{2.303} \tag{5}$$

where q_e and q_t are the values of the amount sorbed per unit mass (mg g^{-1}) at equilibrium and at any time t, respectively and k_l is the pseudo first order Lagergren sorption rate constant (min^{-1}). The k_l values could be obtained by plotting $\log(q_e - q_t)$ versus t for sorption of Be(II) at different temperatures as shown in Fig. 3. The plots show straight lines with good linearity. The values of the first order rate constant (k_l) and correlation coefficient (r^2) obtained from these plots are listed in the Table 1. The values of k_l indicate that the rate of the process increases with temperature.

The calculated correlation coefficients are closer to unity for pseudo first order kinetic model. The calculated equilibrium

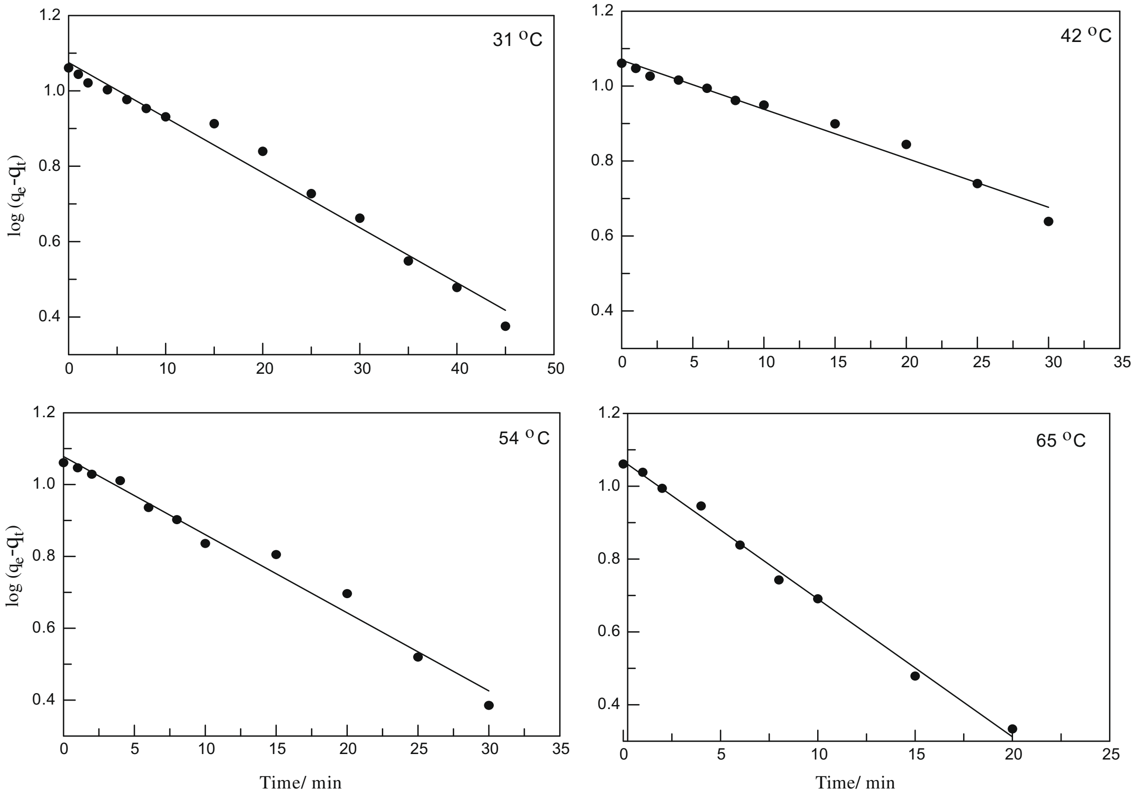

Fig. 3. Lagergren plots for sorption of Be(II) ions onto Amb-IR-120 resin. Amount of resin 0.8 g, shaking speed 150 rpm, pH 3.5.

Table 1
Kinetic parameters for sorption of Be(II) ions by pseudo first order kinetics.

Parameters of Fig. 3	*T*/°C			
	31	42	54	65
Correlation coefficient/r^2	0.97	0.94	0.98	0.99
k_l/min^{-1}	5.61×10^{-4}	5.03×10^{-4}	8.34×10^{-4}	1.45×10^{-3}
q_e/mg g^{-1}	11.89	11.75	11.97	11.72

Table 2
Kinetic parameters for sorption of Be(II) ions by pseudo second order kinetics.

Parameters of Fig. 3	T/°C			
	31	42	54	65
Correlation coefficient/r^2	0.86	0.66	0.45	0.82
k_s/g mg^{-1} min^{-1}	1.61×10^{-5}	4.80×10^{-6}	4.64×10^{-8}	2.51×10^{-5}
q_e/mg g^{-1}	19.61	32.89	38.72	23.26

sorption capacity (q_e) is consistent with the experimental data. Therefore the sorption reaction can be approximated more favorably by the pseudo first order sorption as the predominate mechanism.

In order to insure the description of the kinetics, second order kinetic equation was applied. The pseudo second order kinetics can be represented by the following linear equation [29]

$$\frac{t}{q_t} = \frac{1}{k_s q_e^2} + \frac{t}{q_e} \tag{6}$$

where k_s is the second order rate constant (g mg^{-1} min^{-1}). The kinetic plots of t/q_t versus t for Be(II) removal are shown in Fig. 4. The second order mechanism suffered from inadequacies when applied to Be(II) sorption on the composite sorbents. One of the major discrepancies was observed when q_e values obtained from pseudo second order plots were compared with the experimental q_e values are seen in Table 2. The experimental q_e values differed from the corresponding theoretical values. Thus, the interaction of Be(II) with the synthesized sorbents does not follow second order kinetics.

The obtained data at different temperatures indicated that increasing the temperature increases the adsorption rate process. The activation energy can be determined using Arrhenius equation

$$k = Ae^{-\frac{E_a}{RT}} \tag{7}$$

where A is the pre-exponential factor or simply the prefactor and R is the gas constant. The unit of the pre-exponential factor is identical to that of the rate constant and varies depending on the order of the reaction. Fig. 5 is the Arrhenius plot for the adsorption of Be on Amb-IR-120. The activation energy can be determined from Fig. 5 to be 5.48 ± 0.54 kCal (23.0 ± 2.0 kJ/mol). The results concerning the activation energy indicate diffusion controlled process [30]. As in other heterogeneous reactions between solids and fluids (i.e. between the Be(II) and the Amb-IR-120 ion-exchange resin in our case), the reaction could be explained through a number of sequential processes that determine the rate of reaction: (a) diffusion of ions through the liquid film surrounding the particle. (b) Diffusion of ions through the polymeric matrix of the resin (c) chemical reaction with the functional groups attached to the matrix. One of the steps usually offers much greater resistance than the others so it can be considered as the rate limiting step of the process. There are only a few cases in which the rate of ion-exchange reactions is controlled by chemical reaction. When a kinetic study is in its initial stage, it is generally assumed that the chemical reaction is infinitely fast. Helfferich [31] gives 11 examples in which reactions have an influence on the rate of exchange; they are all related with some kind of parallel ionic reaction that changes the identity of the ions involved. In many cases, ion-exchange kinetics is limited by the step of diffusion inside the resin particle. When convection in the solution is weak and/or the degree of polymer cross-link is low, it is likely that the main resistance to diffusion can be found in the liquid phase. When the degree of cross-linking is high, the resins are more compact, so the mass transfer inside the particles is more difficult.

Homogeneous Particle Diffusion Model (HPDM) is the kinetic model which is widely used to describe the metal adsorption by ion exchange resin. In this model, the extraction mechanism involves counter diffusion of M^{2+} ions from the aqueous solution and H^+ ions from the resin phase through a number of possible resistances. The M^{2+} species originally in the solution phase must diffuse across the liquid film surrounding the ion exchange resin particle, transfer across the solution particle interface, diffuse into the bulk of the ion exchange resin particle and possibly interact with ion exchange reactive group. The species within the ion exchange reactive group simultaneously experience the same sequence in reverse order.

3.3. Data analysis using the homogeneous diffusion model

When the transport of the solute molecules from liquid phase up to solid phase boundary plays the most significant role, the following expression can be used to describe the rate of the ion exchange [32–35]:

$$-\ln(1 - X) = K_{\mathrm{FD}} t \text{ where } K_{\mathrm{FD}} = \frac{3D_{\mathrm{FD}} C_0}{r C_e \delta} \tag{8}$$

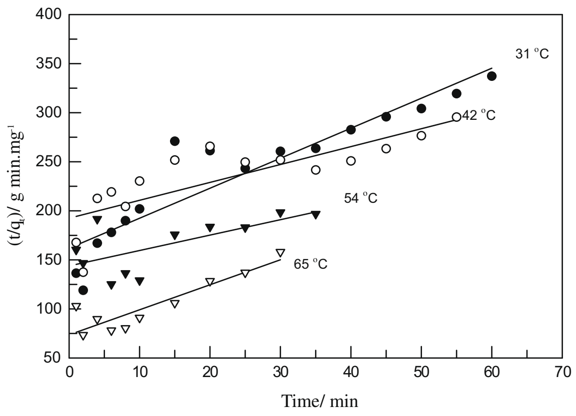

Fig. 4. Pseudo second order plots for sorption of Be(II) ions on Amb-IR-120 resin. Experiment conditions as in Fig. 3.

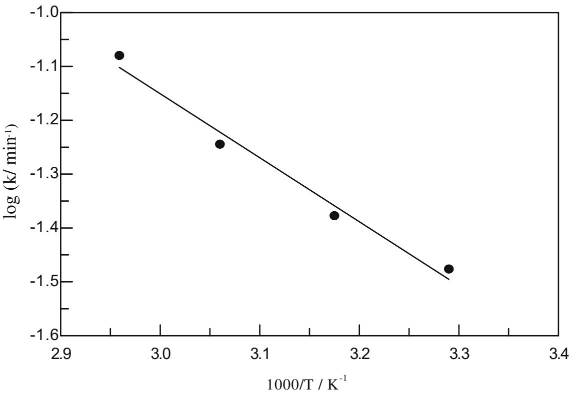

Fig. 5. Arrhenius plot for the sorption of Be(II) ions onto Amb-IR-120.

If matrix phase diffusion controls the rate of exchange, the following analogous expression can be used:

$$-\ln(1-X^2) = 2K_{\mathrm{MD}}\,t \text{ where } K_{\mathrm{MD}} = \frac{\pi^2 D_{\mathrm{MD}}}{r^2} \qquad (9)$$

where X is the fractional attainment of equilibrium ($X = q_t/q_e$). A linear plot of $-\ln(1-X)$ versus time t with zero intercept would suggest that the kinetics of the sorption process is controlled by diffusion through the liquid film surrounding the solid sorbents. Further investigation for the data obtained from batch experiments leads to subdivision of the adsorption process to two stages. Figs. 6(a–d) show the application of the HDM on the experimental data of Be sorption on Amb-IR-120 at different temperatures. The data show different stages (modes) of the controlling diffusion processes. The two main modes were film diffusion mode (FD) and matrix diffusion mode (MD) are given respectively, by Eqs. (8) and (9) above. The experimental data follow FD mode at the beginning of the sorption process (first stage) followed by MD mode after specific time interval (final stage). These specific time intervals depend on the temperature of the solution. For instance, the inflections between the two modes (FD and MD) occur at time of 40, 30, 25, and 15 min at 31, 42, 54, 65 °C, respectively. As the temperature increases the time interval decreases as shown in Figs. 6(a–d). This is consistent with the fact that the rate of the sorption process increases with the temperature as discussed in Section 3.2. As the temperature increases the time required for the ions to exchange onto the solid matrix decreases and hence reaching to the second stage (mode) earlier compared to lower temperatures. The plots at different temperatures as shown in Fig. 6(a–d) indicate that at the first stage the rate determining step is controlled by film diffusion (FD) while at the final stages it is controlled by matrix diffusion (MD). The kinetic parameters for sorption of Be(II) ions according to HDM were estimated using Eqs. (8) and (9) and Figs. 6(a–d) and cited in Table 3. The diffusion coefficients in matrix diffusion (D_{MD}) can be estimated by using $r = 5 \times 10^{-4}$ m in Eq. (9). It increases with temperature. The D_{MD} values were found to be equal 1.90×10^{-11}, 2.56×10^{-11}, 4.10×10^{-11} and 6.05×10^{-11} m^2 s^{-1} at 31, 42, 54, 65 °C respectively. These values may be comparable with those found for Cr(III) (4.2×10^{-12} m^2 s^{-1}) and Zn(II) (6.2×10^{-12} m^2 s^{-1}) [36]. On the other hand, the K_{FD} values in Table 3 indicate that the

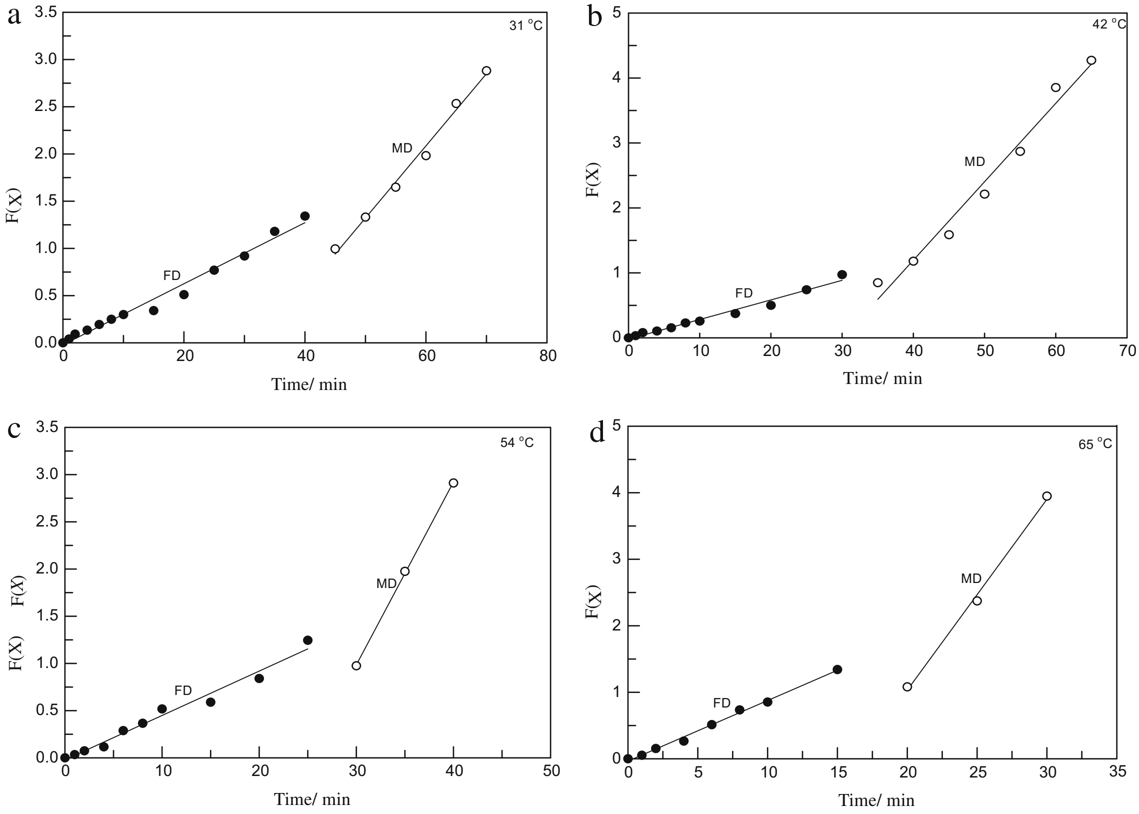

Fig. 6. (a–d) Homogenous diffusion mode plots for sorption of Be(II) ions on Amb-IR-120 resin at different temperatures. FD holds for film diffusion mode given by Eq. (8) and MD holds for matrix diffusion mode given by Eq. (9).

Table 3
Estimated parameters for sorption of Be(II) ions from plots of the homogenous diffusion model shown in Fig. 6a–d. Kinetic parameters for sorption of Be(II) ions homogenous diffusion model.

Parameters of Fig. 6(a–d)	T/°C							
	31		42		54		65	
	FD	MD	FD	MD	FD	MD	FD	MD
Correlation coefficient/r^2	0.98	0.99	0.98	0.98	0.98	0.99	0.99	0.99
K_{FD}/S^{-1}	5.4×10^{-4}		5.02×10^{-4}		7.83×10^{-4}		1.52×10^{-3}	
K_{MD}/S^{-1}		7.5×10^{-4}		1.01×10^{-3}		1.62×10^{-3}		2.39×10^{-3}

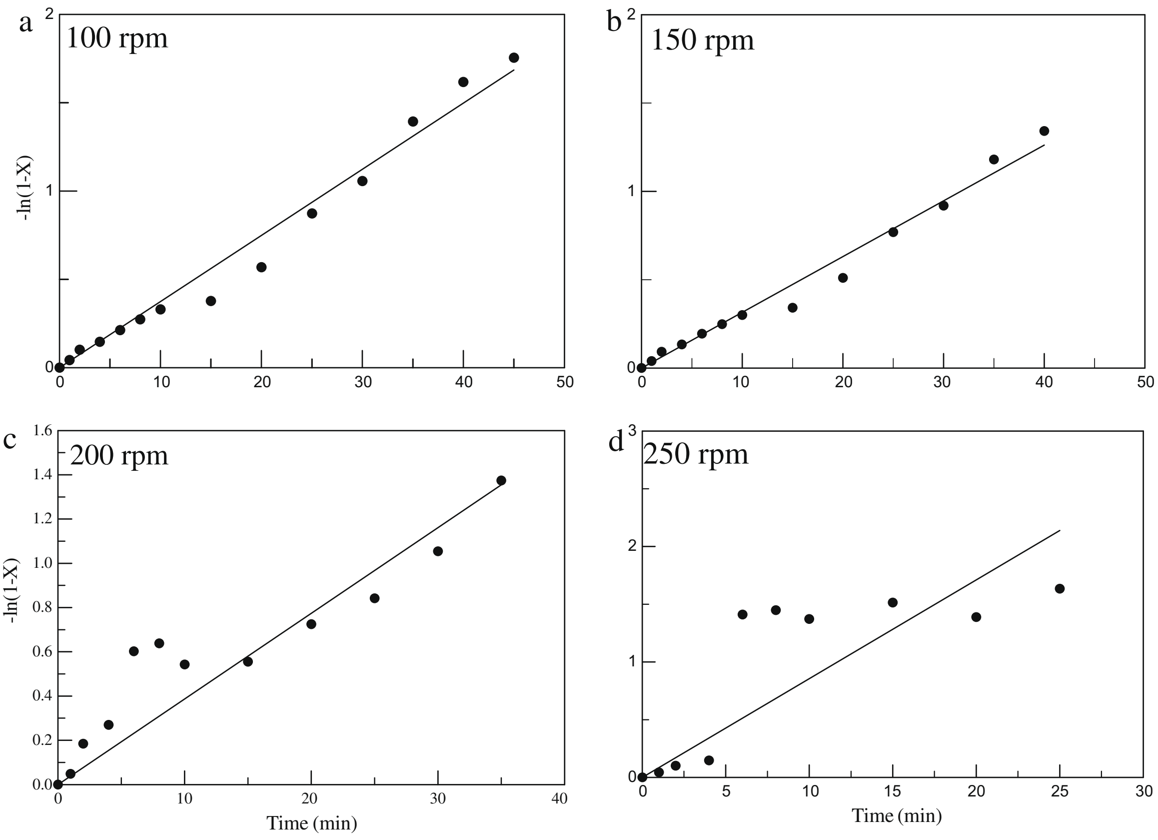

Fig. 7. (a–d) Effect of shaking speed on the liquid film diffusion of the absorption of Be(II) on Amb-IR-120 resin. Amount of resin 0.8 g, pH 3.5, at 31 °C.

diffusion coefficient in the liquid film, D_{FD} increases with the temperature (assuming a constant value of the film thickness δ). This is consistent with the fact that the rate of the process reaching to the second stage earlier at higher temperatures.

3.4. Effect of the rate of agitation

Further investigations of the two stages of adsorption are conducted by studying the effect of the rate of agitation. The experiment are carried out at stirring speed ranged between 100 and 250 rpm at 31 °C for 10 min. Figs. 7 and 8 show the application of the HDM equation on the collected experimental data for sorption of Be at different shaking speed (rpm). In Figs. 7(a–d) the FD equation (Eq. (8)) was applied for the sorption process at the early stage. The strategy which has been done with Fig. 6 was applied here too. That is to say, the data in Fig. 7 represent the early stage where as Fig. 8 represent the final stage of the process. Fig. 7(a) and (b) follow Eq. (9) and relatively good straight lines were obtained with respect to the unsatisfactory straight lines obtained in Fig. 7(c) and (d). The above results imply that FD model can describe the sorption process at lower shaking speed where diffusion of Be^{2+} from bulk solution to the sorbent surface is the controlling process. In Fig. 8 the data at the final stage (i.e. after specific time interval similar to those in Fig. 6) applied to the matrix diffusion equation (Eq. (9)) and satisfactory straight lines are obtained. It is evident from Fig. 8 that the second mode (stage 2) (i.e. DM) begins earlier than at lower shaking speed. At higher shaking speed the FD is not controlling and yet the matrix diffusion controls the process faster than at lower shaking speed.

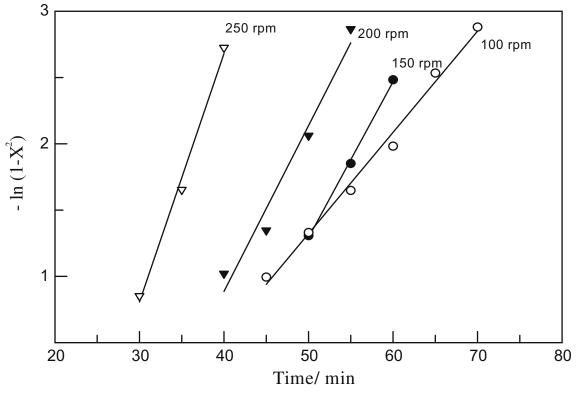

Fig. 8. Effect of shaking speed on the matrix diffusion of the absorption of Be(II) on Amb-IR-120 resin. Experiment conditions are the same as in Fig. 7.

The data analysis according to homogeneous diffusion model confirms the concept of the two stages of diffusion. As shown in Figs. 7 and 8, at low rate of agitation the rate determining step is a combination of film and matrix control while at high rate of agitation only matrix diffusion controls the process.

4. Summary and conclusions

We have used the equations of the homogenous diffusion model (HDM) and the two-stage concept of the diffusion to fit our experimental data. Results obtained in this work on the kinetics adsorption of Be(II) with Amberlite-IR-120 resins have indicated that:

- At the early stage of the process, the sorption is fast and the rate-determining step of the metal extraction is the liquid-film diffusion.

- At the final stage of the process, the sorption is slow and the rate-determining step of the metal extraction is the matrix (resin)-phase diffusion
- Both the model and the two-stage concept allow the estimation of the average diffusion coefficient which provides an insight into the diffusion mechanism and a parameter for subsequent design calculations.
- The kinetic parameters obtained are of the same order of magnitude as those measured by other authors when dealing with heterogeneous chemical adsorption reaction and are higher than those obtained with physical adsorption reaction. This fact gives an indication of the high affinity of Be(II) towards Amberlite-IR-120 resin.

As a final conclusion, the two stages of diffusion mechanisms represent reasonable approaches to the kinetics of the metal extraction reactions on polymeric macroporous ion exchange resin. The present situation calls for more complicated mathematical modeling for better understanding and optimization of the sorption of Be^{2+} on Amb-IR-120. The above findings on batch process will be applied using a fixed-bed column and will be reported in the near future.

References

[1] M.E. Kolanz, Appl. Occup. Environ. Hyg. 16 (2001) 559.
[2] Tammy P. Taylor, Nancy N. Sauer, J. Hazard. Mater. 93 (2002) 271.
[3] E.G. Tsvetkov, G.M. Rylov, V.N. Matrosov, Mater. Res. Bull. 41 (2006) 307.
[4] V.V. Gurov, E.G. Tsvetkov, A.G. Kirdyashkin, J. Cryst, Growth 256 (2003) 361.
[5] E.V. Pestryakov, V.V. Petrov II, V.I. Zubrinov, V.I. Semenov, A.V. Trunov, J. Kirpichnikov, J. Appl. Phys. 82 (1997) 3661.
[6] A.I. Alimpiev, V.S. Gusev, P.W. Mokrushnikov, Cryst. Res. Technol. 30 (1995) 295.
[7] G.S. Brady, Materials Handbook, 3rd Ed., McGraw-Hill Inc., San Francisco, 1971.
[8] G. Choppin, J. Liljenzin, J. Rydberg, Radiochemistry and Nuclear Chemistry, 3rd Ed., Butterworth-Heinemann, USA, 2002.
[9] A.F. Crooks, P.J. Abbott, Beryl in South Australia, South Australia, Department of Primary, Industries and Resources, Report Book, 2004/25, 2004.
[10] I. Nukatsuka, K. Sakai, R. Kudo, K. Ohzeki, Analyst 120 (1995) 2819.
[11] E. Merian (Ed.), Carcinogenic and Mutagenic Metal Compounds, vol. 11, VCH Publishers, New York, 1991, p. 775.
[12] B.J. Alloway, D.C. Ayres (Eds.), Chemical Principles of Environmental Pollution, 2nd Ed., Blackie Academic and Professional, London, 1997, p. 49.
[13] M. Bettinelli, S. Spezia, U. Baroni, G. Bizzarri, Atom. Spectrosc. 19 (1998) 73.
[14] H. Lachas, R. Richaud, K.E. Jarvis, A.A. Herod, D.R. Dugwell, R. Kandiyoti, Analyst 124 (1999) 177.
[15] C. Neal, Sci. Total Env. 314 (2003) 171.
[16] M.J. Shaw, S.J. Hill, P. Jones, P.N. Nesterenko, Chromatographia A876 (2000) 127.
[17] T. Okutani, Y. Tsuruta, A. Sakuragawa, Anal. Chem. 65 (1993) 1273.
[18] S.E. Manhan, Environmental Chemistry, 6th Ed., Lewis Publishers, Ann Arbor, 1994.
[19] M. Sitting, Hand Book of Toxic and Hazardous Chemicals and Carcinogens, 2nd Ed., Noyes Publications, New Jercy, 1985.
[20] USEPA, Technology Transfer Network, Beryllium and Compounds, Office of Air Quality Planning and Standards, Research Triangle Park, North Carolina, 1998, 107-02-8.
[21] G.M. Milton, W.E. Grummitt, Can. J. Chem. 35 (1957) 541.
[22] W.D. Ehmann, T.P. Kohman, Geochim. et Cosmochim. Acta 14 (1958) 340.
[23] M.N. Nadkarni, M.S. Varde, V.T. Athavale, Anal. Chim. Acta 16 (1957) 421.
[24] E.G. Owens II, J.H. Yoe, Anal. Chem. 32 (1960) 1345.
[25] N. Swami, D.B. Dreisinger, Solvent Extr. Ion Exch. 13 (1995) 1037.
[26] S. Gonzalez-Luque, M. Streat, Hydrometallurgy 11 (1983) 227.
[27] R.R. Sheha, A.A. El-Zahhar, J. Hazard. Mater. 150 (2008) 795.
[28] R.R. Sheha, J. Colloid Interf. Sci. 310 (2007) 18.
[29] Y.S. Ho, G. McKay, Process Biochem. 34 (1999) 451.
[30] M.M. Saleh, Water Research 40 (2006) 1052.
[31] F. Helfferich, in: Ion-exchange, McGraw-Hill, New York, USA, 1962.
[32] S. Gonzalez-Luque, M. Streat, Hydrometallurgy 11 (1983) 207.
[33] J.L. Cortina, N. Miralles, Solv. Extr. Ion Exch. 15 (1997) 1067.
[34] L. Liberti, R. Passino, in: J.A. Marinsky, Y. Marcus (Eds.), Ion Exchange and Solvent Extraction, vol. 7, Marcel Dekker Inc., NewYork, 1977 (Chapter 3).
[35] F. Helfferich, Ion-exchange, Mc Graw-Hill, New York, USA, 1962.
[36] Vitor J.P. Vilar, Cidalia M.S. Botelho, Rui A.R. Boaventura, J. Hazard. Mater. 149 (2007) 643.